HHS Public Access

Author manuscript

Biochem Biophys Res Commun. Author manuscript; available in PMC 2016 December 25.

Published in final edited form as:

Biochem Biophys Res Commun. 2015 December 25; 468(4): 719–725. doi:10.1016/j.bbrc.2015.11.022.

Blockade of Drp1 rescues oxidative stress-induced osteoblast dysfunction

Xueqi Gan[a,b,1], **Shengbin Huang**[a,b,1], **Qing Yu**[a,b], **Haiyang Yu**[b], and **Shirley ShiDu Yan**[a,*]

[a]Department of Pharmacology and Toxicology and Higuchi Bioscience Center, University of Kansas, Lawrence, KS, 66047, USA

[b]State Key Laboratory of Oral Diseases, West China Hospital of Stomatology, Sichuan University, Chengdu, 610041, China

Abstract

Osteoblast dysfunction, induced by oxidative stress, plays a critical role in the pathophysiology of osteoporosis. However, the underlying mechanisms remain unclarified. Imbalance of mitochondrial dynamics has been closely linked to oxidative stress. Here, we reveal an unexplored role of dynamic related protein 1(Drp1), the major regulator in mitochondrial fission, in the oxidative stress-induced osteoblast injury model. We demonstrate that levels of phosphorylation and expression of Drp1 significantly increased under oxidative stress. Blockade of Drp1, through pharmaceutical inhibitor or gene knockdown, significantly protected against H_2O_2-induced osteoblast dysfunction, as shown by increased cell viability, improved cellular alkaline phosphatase (ALP) activity and mineralization and restored mitochondrial function. The protective effects of blocking Drp1 in H_2O_2-induced osteoblast dysfunction were evidenced by increased mitochondrial function and suppressed production of reactive oxygen species (ROS). These findings provide new insights into the role of the Drp1-dependent mitochondrial pathway in the pathology of osteoporosis, indicating that the Drp1 pathway may be targetable for the development of new therapeutic approaches in the prevention and the treatment of osteoporosis.

Keywords

Osteoblast; Osteoporosis; Oxidative stress; Drp1; Mitochondrial function; Reactive oxygen species

1. Introduction

Osteoporosis is one of the most prevalent degenerative diseases affecting elderly people [1,2] and is characterized by low bone mass, altered bone microarchitecture and increased

*Corresponding author. Departments of Pharmacology and Toxicology and Higuchi Bioscience Center, School of Pharmacy, University of Kansas, 2099 Constant Ave., Lawrence, KS 66047, USA. shidu@ku.edu (S.S. Yan).

1These author contribute equally to this work.

Conflict of interest

The authors declare no competing financial interests.

Transparency document

Transparency document related to this article can be found online at http://dx.doi.org/10.1016/j.bbrc.2015.11.022.

risk of fracture [1,2]. Multiple factors have been implicated in the development of osteoporosis, including gender, age, body weight, sustained glucocorticoid therapy and endocrinological disorders [1,3]. Recently, the “estrogen-centric” account of pathogenesis has been supplanted by an account where oxidative stress is recognized as a protagonist in the development of osteoporosis [4]. The detailed mechanisms by which oxidative stress affects bone property are not well understood [5].

Osteoblasts are responsible for bone formation, whilst osteoclasts participate in bone resorption. Conditions such as osteoporosis are associated with significant changes in bone turnover: bone formation decreases whilst bone resorption increases or remains the same, resulting in net bone loss [6,7]. Increasing evidence has demonstrated that insufficient osteogenesis resulting from oxidative stress-induced osteoblast dysfunction is an important cause of bone loss in the pathology of osteoporosis [8,9]. Moreover, increased oxidative stress may contribute to the inhibition of osteoblast differentiation [10] and proliferation [11] or the induction of cell death [12,13]. The specific mechanisms and key players by which oxidative stress induces osteoblast dysfunction need to be further elucidated.

Oxidative stress, resulting from excessive generation of reactive oxygen species (ROS), could damage all cellular components [14]. Mitochondria are the main source of ROS and also the principal target of ROS attacks. The damaged mitochondria accumulate under conditions of oxidative stress, suggesting that maintaining a pool of healthy mitochondria is crucial for protecting against pathological conditions including Alzheimer’s disease (AD) [15] and diabetes [16]. Furthermore, mitochondria are dynamic organelles, which undergo continuous fission and fusion. A line of evidence demonstrated that ROS production is correlated with increased fission [17–22]. In these settings, oxidative stress is causative for mitochondrial fragmentation; therefore, fission might represent a strategy to cope with oxidative stress. However, under hyperglycemic conditions such as those present in diabetes, mitochondria undergo Drp1-dependent fission, resulting in increased ROS release and production, suggesting that fission also contributes to ROS-mediated cellular perturbation [23]. In our previous study, we demonstrated that the treatment with antioxidant protects against AD-induced mitochondrial fission-fusion imbalances, while blockade of the mitochondrial fission protein Drp1 by a genetic manipulation or pharmacological inhibition effectively attenuates the effect of oxidative stress in AD cybrid cells [20,21]. These studies indicate the role of Drp1 in the oxidative stress-induced cellular perturbation and injury and preset Drp1as a potential novel therapeutic target for prevention or treatment of oxidative stress-related diseases. So far, it is unknown whether mitochondrial fusion and fission events are involved in the process of osteoblast dysfunction insulted by oxidative stress and whether blockade of Drp1prevents or rescues osteoblast dysfunction-induced by oxidative stress. The present study is to investigate the effect of Drp1 on oxidative stress-induced osteoblast function in a human osteoblast cell model. The outcome of the results will deepen our understanding of the impact of Drp1-related perturbations on mitochondrial function and add to the body of literature on Drp1-dependent mechanisms underlying oxidative stress–mediated cell injury relevant to osteoblast structure and function.

2. Material and methods

2.1. Cell culture

Human Sao-2 cells (obtained from ATCC) were cultured in α-minimum essential medium (α-MEM), supplemented with 10% fetal bovine serum (FBS) and 1% penicillin streptomycin in 5% CO_2 at 37 °C. This basic medium was replenished twice a week. For induction of osteogenetic differentiation, β-glycerophosphate (5 mM) and ascorbic acid (100 μg/mL) were added to basic culture medium.

2.2. Cell treatment

Drugs were prepared as stock solutions and were diluted to a final concentration immediately before use. Final concentration and sources of the drugs were as follows: H_2O_2 (100 μM) mdivi-1 (10 μM). The final concentration of vehicle control dimethyl sulfoxide (DMSO) was less than 0.5% in all experiments. Cells were treated with or without H_2O_2 and specific inhibitors for various times in the basic medium or differentiation medium. On the other hand, cells were transfected with plasmids containing GFP-tagged Drp1 K38A (provided by Dr. Yi-Ren Hong, Kaohsiung Medical University Hospital, Taiwan) or empty control vectors using Lipofectamine 2000 (Invitrogen) according to manufacturer's instructions. To knockdown expression of Drp1, cells were transfected with siRNA targeting human Drp1 or control siRNA using Oligofectamine. After transfection, the efficiency was evaluated by immunoblotting of Drp1 protein and cells were treated with the indicated reagents and assessed for changes in viability and osteoblast function.

2.3. Cell viability assay

Osteoblasts were plated at 10^4 cells/well in 96-well plates and cultured under variable conditions as indicated. Cell viability assay at different periods of time (24, 48, 96 h) was conducted by MTT (3-(4,5-dimethylthiazol-2-yl)-2,5-diphenyltetrazolium bromide method. In brief, osteoblasts in 96 well plates were washed twice with 0.01 M PBS, and then incubated in 100 μl of FBS-free α-MEM supplemented with 10 μl of 5 mg/ml MTT solution at 37 °C. After 4 h incubation, the supernatant was carefully removed, and the crystals were dissolved by incubation with 150 μl of DMSO for 20 min. The plates were shaken for 15s and then absorbance at 570 nm was measured in a micro plate reader (Molecular device).

2.4. Alkaline phosphatase (ALP) activity assay and ALP staining

The osteoblasts were seeded at 105 cells/well in 12-well plates and stimulated with differentiation medium for 1 week. The cells were then serum-deprived overnight and incubated with indicated reagents for 3 days. ALP activity in the cell lysate was assayed at the end of the incubation time with 10mMp-nitrophenyl phosphate in 0.15 M sodium carbonate buffer (pH 10.3) and 1 mM $MgCl_2$ as described. The enzyme activity was normalized against the cellular protein concentration and expressed as U/g protein. Protein concentration was determined using Bradford protein assay.

ALP staining was performed by a standard protocol. In brief, cells cultured on glass slides were fixed with 4% PFA and subjected to ALP staining using ALP kit according to the manufacture's instruction.

2.5. Mineralization assay

Cells were seeded at 105 cells/well in 12-well plates and were stimulated with osteogenic differentiation medium with indicated reagents for 3 weeks. The medium was replenished twice a week. To detect calcification, cells were fixed with 4% PFA and stained with Alizarin red according to the manufacture's instruction.

2.6. Protein extraction and Western blot analysis

Osteoblasts cultured in different conditions were lysed with RIPA buffer. Proteins were electrophoresis by SDS-PAGE and transferred to membrane. Anti-phospho-Drp1 (1:3000, cell signaling), anti-Drp1 (1:3000, BD Science) and anti-β-actin (1:5000, Sigma) were used as primary antibodies. The binding sites of primary antibody were visualized with horseradish peroxidase-conjugated anti-rabbit IgG antibody (1:5000, Invitrogen) or anti-mouse IgG antibody(1:5000, Invitrogen), followed by the addition of ECL substrate. The immunoreactive band relative to optical density was determined by using NIH Image J software (public domain) and normalized with β-actin levels.

2.7. Mitochondrial respiratory enzyme activity measurement

Mitochondrial respiration complex activity was measured in osteoblast homogenates according to our previous studies [15,16]. In brief, osteoblast cultures in six well plates were washed with ice-cold PBS, harvested, centrifuged, and suspended in 50 μl of isolation buffer (225 mM D-mannitol, 75 mM sucrose, 2 mM K_2HPO_4, 5 mM HEPES, pH 7.2). 10–50 μg mitochondrial fractions were used for complex activity assay. Enzyme activities of complex I (NADH ubiquinone oxidoreductase), complex III (ubiquino cytochrome C oxidoreductase), and complex IV (cytochrome C oxidase, or CcO) were determined as described.

2.8. Functional image assay

Osteoblasts were seeded in chamber slides at a density of 10^4 cells/well. Cells were treated with/without H_2O_2, mdivi-1 for 1 h. To detect mitochondrial superoxide production, utilization of Mitosox Red, a unique fluorogenic dye used for a highly selective detection of superoxide production in the mitochondria of live cells was chosen. Cells were incubated with fresh basic medium containing 2.5 μM Mitosox for 30 min.

Mitochondria were labeled with Mitotracker Red (Molecular Probes, incubated in 100 nM Mitotracker Red for 30 min at 37 °C before fixation to visualize morphology. Images were captured under a confocal microscope (Leica TCS SPE). Excitation wavelengths were 543 nm for Mitosox, TMRM or Mitotracker Red, and 488 nm for MTGreen, respectively. Post-acquisition processing was performed with MetaMorph (Molecular Devices) and NIH Image J software for quantification and measurement of fluorescent signals of mitochondrial length and occupied area. Mitochondrial size, density, and fluorescent intensity were quantified by an investigator blinded to experimental groups. More than 100 clearly identifiable mitochondria from 10 to 15 randomly selected cells per experiment were measured in 3 independent experiments.

2.9. Statistical analysis

Data are presented as mean ± SEM (the standard error of the mean). Statistical analysis was performed using Statview software (SAS Institute, Version 5.0.1). Differences between means were assessed by Student's t-test or one-way analysis of variance (ANOVA) with Fisherposthoc test. $P < 0.05$ was considered significant.

3. Results

3.1. Oxidant (H_2O_2)-induced osteoblast dysfunction

We found that H_2O_2 treatment at a concentration of 100 μM induced oxidative stress and cellular dysfunction. Therefore, we used this model in the following experiment. Compared with the vehicle-treated control group, treatment with H_2O_2 significantly decreased cell viability of osteoblasts in a time-dependent manner (Fig. 1A). Cellular ALP activity (Fig. 1B), expression of ALP (Fig. 1C), and mineralization (Fig. 1D) were also significantly suppressed by H_2O_2 treatment. These results are consistent with the previous observation that H_2O_2 toxicity leads to osteoblast dysfunction.

3.2. Oxidant (H_2O_2) mediated mitochondrial dysfunction

Mitochondria are a major source of ROS generation and H_2O_2 treatment has served as classical oxidative stress model. Therefore, we evaluated whether increased oxidative stress exacerbated mitochondrial dysfunction by examining mitochondrial ROS and key enzyme activity associated with mitochondrial respiratory function. Using highly selective fluorescent dye (Mitosox) to detect mitochondria-derived ROS, we observed that the intensity of Mitosox staining was significantly increased in osteoblasts treated with H_2O_2 (Fig. 1E–F), suggesting that H_2O_2 induced high levels of ROS within the mitochondria of osteoblasts.

Oxidative phosphorylation enzyme complexes play the essential roles in physiological mitochondrial functions; thus, the key enzymes associated with respiratory chains were evaluated in this study. Compared to the control group, the presence of H_2O_2 significantly decreased the activity of complex III and IV (Fig 1. G–H).

3.3. H_2O_2 caused osteoblast mitochondrial fragmentation

In view of increased mitochondrial ROS in H_2O_2-treated osteoblasts, the important contribution of oxidative stress to mitochondrial dysfunction, and abnormal changes in mitochondrial structure, we next determined if oxidative stress affects mitochondrial morphology and fission/fusion dynamics in the osteoblast oxidative stress model. Morphologically, mitochondria in the control group were rod-like or elongated and regularly distributed, whereas mitochondria were fragmented, misshapen, bleb-like and collapsed away from the mitochondrial network in the oxidative stress model (Fig. 1I). Compared with the control group, mitochondrial density and length significantly decreased in the presence of H_2O_2 (Fig. 1J–K).

Given that imbalance of mitochondrial fission and fusion plays a critical role in the maintenance of mitochondrial morphology, distribution and function, we next investigated if

mitochondrial dynamics were altered in the oxidative stress model. Phosphorylation of Ser616 on Drp1 is critical for mitochondrial fission [16]. We observed an increase in Ser616 phosphorylation in parallel with increased total Drp1 expression in osteoblasts treated with H_2O_2 (Fig. 1L–N). These results suggest increased mitochondrial fission occurs in osteoblasts insulted by oxidative stress, which may subsequently impair mitochondrial morphology and function.

3.4. Inhibiting excessive mitochondrial fission restores mitochondrial morphology and function

We evaluated whether inhibition of excessive mitochondrial fission via targeting Drp1, a key protein controlling mitochondrial fission, protected against oxidative stress-induced aberrant mitochondrial morphology and function. Treatment with mdivi-1, a selective inhibitor of Drp1 activity, significantly increased mitochondrial length and density in osteoblasts, as compared to vehicle-treated control osteoblasts (Fig. 2A–C). Furthermore, genetic inactivation of Drp1 with dominant-negative Drp1 (DN-Drp1) (Fig. 2D–F) or knockdown of Drp1 with siRNA-Drp1 (Fig. 2G–I) also protected mitochondrial morphology and dynamics from the adverse effect of H_2O_2. In the area of mitochondrial function, as shown in Fig. 3, treatment with mdivi-1 significantly suppressed ROS production (Fig. 3A–B). Consistent with these results, the addition of mdivi-1, inactivation of Drp1 and knockdown of Drp1 enhanced complex III (Fig. 3C–E) and CcO activity (Fig. 3F–H). These results indicate that Drp1-mediated excessive mitochondrial fission potentiates osteoblast mitochondria abnormalities under oxidative stress.

3.5. Drp1 inhibition restores osteoblast function

Next, we evaluate whether oxidative stress-induced alterations in mitochondrial fission and function interfere with osteoblast function. The addition of mdivi-1 significantly increased ALP activity (Fig. 4A and C) and bone node formation (Fig. 4B), as compared with the vehicle-treated control in the presence of H_2O_2. Furthermore, genetic knockdown of Drp1 significantly enhanced ALP activity, as compared with cells treated with control siRNA treatment (Fig. 4D). These data demonstrate that blockade of Drp1 attenuates oxidative stress-induced osteoblast dysfunction.

4. Discussion

Although oxidative stress induced osteoblast dysfunction is recognized as a crucial initiating factor in the development and progression of osteoporosis, the underlying mechanisms are not well understood [24]. Multiple lines of evidence suggest that alterations in mitochondrial dynamics are closely linked to oxidative stress [25–27], however, few studies have been conducted to investigate these links as related to osteoblast dysfunction induced by oxidative stress. In the present study, we investigate the effect of Drp1, a major fission generator, on oxidant-induced osteoblast dysfunction. The results revealed that Drp1 is involved in oxidative stress-induced mitochondrial dysfunction, leading to osteoblast injury. Blockade of Drp1 protects against oxidative stress-induced deleterious effects on cell survival, mitochondrial function, osteogenic formation, osteoblast differentiation. Our current study

reveals the role of Drp1 in oxidative stress-induced osteoblast dysfunction, which may contribute to the development and progression of osteoporosis.

In the present study, the viability of osteoblasts was significantly reduced under H_2O_2 treatment, which became more obvious with increasing exposure time. Moreover, oxidative stress not only affects cell viability, but it also affects differentiation, as seen in the results of the ALP activity test and calcium mineralization investigation. These results were consistent with previous reports that age-related bone loss in humans and animals is due mainly to a deficit in osteoblasts resulting from the reduced osteoblast ogenesis or increased apoptosis relevant to increased oxidative stress [28].

Given that the imbalance of mitochondrial fission and fusion plays a critical role in maintenance of mitochondrial morphology, distribution and function, we investigated if mitochondrial dynamics were altered in the process of oxidative stress-induced osteoblast dysfunction and we assessed the link between oxidative stress and changes in mitochondrial dynamics. Obviously, treatment with H_2O_2 resulted in more fragmentation of mitochondria in osteoblasts, in addition to an increase in Ser616 phosphorylation and total of Drp1 expression levels. Notably, blockade of Drp1to inhibit oxidative stress-induced excessive mitochondrial fission significantly suppressed oxidative stress-induced reduction in their osteogenic differentiation ability, as demonstrated by preserved ALP activity and formation of mineralized nodules upon oxidative stress condition. These results suggest that Drp1-dependent fission is involved in oxidative stress-induced mitochondrial perturbation contributing to osteoblast dysfunction. The detailed mechanisms underlying Drp1-involved osteoblast function, including bone mineralization, formation, and differentiation, requires further investigation.

Mitochondria are now recognized as unique and irreplaceable organelles in eukaryotic cells, which not only act as a power plant for energy production, but also play important roles in cell death, function, and survival [29]. In osteoblasts, mitochondria are specialized for calcium transport and are important in the calcification of the extracellular matrix [30]. Moreover, mineral formation has been demonstrated in matrix vesicles and within mitochondria. Release of mitochondrial calcium occurs concomitantly with mineral ion loading of matrix vesicles at the onset of mineralization. Mitochondrial respiratory chain complexes also regulate mineralization [31]. Therefore, mitochondrial dysfunction in osteoblasts is directly or indirectly implicated in osteoporosis. In the oxidative stress model we used, we clearly found that the mitochondrial membrane potential and respiratory chain complex activity were significantly reduced in conditions where production of mitochondrial ROS was significantly up-regulated. This result is consistent with that from a previous study using MC3T3-E1 osteoblasts, where complex IV activity was reduced [32]. Furthermore, to determine whether mitochondrial fission is required for activation-induced ROS generation in osteoblasts, we examined the effect of Drp1 inhibition using a pharmacological Drp1 inhibitor (mdivi-1). Pretreatment with mdivi-1 significantly suppressed mitochondrial ROS accumulation and production, suggesting anti-oxidant properties for mdivi-1, which might explain (to a certain degree) the protective effects of Drp1 inhibition on H_2O_2-induced reduction of osteogenic differentiation and mineralization potentials. The oxidative stress-

induced mitochondrial defects were also reversed by the introduction of DN-Drp1 and siRNA-mediated down regulation in addition to mdivi-1.

As stated above, mitochondrial function is relevant to osteoblast function including proliferation and differentiation. Drp1 inhibition attenuated abnormal mitochondrial morphology and improved mitochondrial function, which protected osteoblasts from oxidative stress injury. Furthermore, mitochondrial dysfunction has been linked to oxidative stress and blockade of Drp1 by pharmaceutical inhibitors or genetic knockdown of Drp1rescued mitochondrial dysfunction in osteoblasts, which further reduced ROS production. Taken together, our data support that Drp1 plays a critical role in the mitochondrial dynamic imbalance resulting from insults by oxidative stress in osteoblasts. The protective effect of Drp1 inhibition in an oxidative stress-mediated cellular injury model suggests that Drp1 may represent a potential and novel target for osteoporosis.

5. Conclusion

The present study demonstrated that oxidative stress induces osteoblast dysfunction via the Drp1-dependent pathway. Blockade of excessive mitochondrial fission attenuates oxidative stress-mediated osteoblast injury (Fig. 4E). Thus, targeting Drp1 may be a significant novel therapeutic strategy for osteoporosis.

Acknowledgments

This study was supported by National Institutes of Health (NIH).

References

1. Zhao Y, Liu Y, Zheng Y. Osteoporosis and related factors in older females with skeletal pain or numbness: a retrospective study in East China. J Int Med Res. 2013; 41:859–866. [PubMed: 23685891]
2. Khosla S, Melton LJ 3rd, Riggs BL. The unitary model for estrogen deficiency and the pathogenesis of osteoporosis: is a revision needed? J Bone Mineral Res Off J Am Soc Bone Mineral Res. 2011; 26:441–451.
3. Compston JE. Risk-factors for osteoporosis. Clin Endocrinol. 1992; 36:223–224.
4. Manolagas SC. From estrogen-centric to aging and oxidative stress: a revised perspective of the pathogenesis of osteoporosis. Endocr Rev. 2010; 31:266–300. [PubMed: 20051526]
5. Yang YH, Zheng XF, Li B, Jiang SD, Jiang LS. Increased activity of osteocyte autophagy in ovariectomized rats and its correlation with oxidative stress status and bone loss. Biochem Biophys Res Co. 2014; 451:86–92.
6. Isomura H, Fujie K, Shibata K, Inoue N, Iizuka T, Takebe G, Takahashi K, Nishihira J, Izumi H, Sakamoto W. Bone metabolism and oxidative stress in postmenopausal rats with iron overload. Toxicology. 2004; 197:93–100. [PubMed: 15003320]
7. Yalin S, Comelekoglu U, Bagis S, Sahin NO, Ogenler O, Hatungil R. Acute effect of single-dose cadmium treatment on lipid peroxidation and antioxidant enzymes in ovariectomized rats. Ecotoxicol Environ Safe. 2006; 65:140–144.
8. Jiang SD, Yang YH, Chen JW, Jiang LS. Isolated osteoblasts from spinal cord-injured rats respond less to mechanical loading as compared with those from hindlimbimmobilized rats. J Spinal Cord Med. 2013; 36:220–224. [PubMed: 23809592]
9. Harada S, Rodan GA. Control of osteoblast function and regulation of bone mass. Nature. 2003; 423:349–355. [PubMed: 12748654]

10. Mody N, Parhami F, Sarafian TA, Demer LL. Oxidative stress modulates osteoblastic differentiation of vascular and bone cells. Free Radic Biol Med. 2001; 31:509–519. [PubMed: 11498284]
11. Li M, Zhao L, Liu J, Liu AL, Zeng WS, Luo SQ, Bai XC. Hydrogen peroxide induces G(2) cell cycle arrest and inhibits cell proliferation in osteoblasts. Anat Rec. 2009; 292:1107–1113.
12. Almeida M, Han L, Ambrogini E, Bartell SM, Manolagas SC. Oxidative Stress Stimulates Apoptosis, Activates NF-kappa, B in osteoblastic cells via a PKC beta/p66(shc) signaling cascade: counter regulation by estrogens or androgens. Mol Endocrinol. 2010; 24:2030–2037. [PubMed: 20685851]
13. Almeida M, Martin-Millan M, Ambrogini E, Bradsher R, Han L, Chen XD, Roberson PK, Weinstein RS, O'Brien CA, Jilka RL, Manolagas SC. Estrogens attenuate oxidative stress and the differentiation and apoptosis of osteoblasts by dna-binding-independent actions of the ER alpha. J Bone Mineral Res. 2010; 25:769–781.
14. Arias-Loza PA, Muehlfelder M, Pelzer T. Estrogen and estrogen receptors in cardiovascular oxidative stress. Pflug Arch Eur J Physiol. 2013; 465:739–746.
15. Gan XQ, Huang SB, Wu L, Wang YF, Hu G, Li GY, Zhang HJ, Yu HY, Swerdlow RH, Chen JX, Yan SS. Inhibition of ERK-DLP1 signaling and mitochondrial division alleviates mitochondrial dysfunction in Alzheimer's disease cybrid cell. Bba Mol Basis Dis. 2014; 1842:220–231.
16. Huang SB, Wang YF, Gan XQ, Fang D, Zhong CJ, Wu L, Hu G, Sosunov AA, McKhann GM, Yu HY, Yan SS. Drp1-mediated mitochondrial abnormalities link to synaptic injury in diabetes model. Diabetes. 2015; 64:1728–1742. [PubMed: 25412623]
17. Fan XY, Hussien R, Brooks GA. H_2O_2-induced mitochondrial fragmentation in C2C12 myocytes. Free Radic Bio Med. 2010; 49:1646–1654. [PubMed: 20801212]
18. Jendrach M, Mai S, Pohl S, Voth M, Bereiter-Hahn J. Short- and long-term alterations of mitochondrial morphology, dynamics and mtDNA after transient oxidative stress. Mitochondrion. 2008; 8:293–304. [PubMed: 18602028]
19. Wu SN, Zhou FF, Zhang ZZ, Xing D. Mitochondrial oxidative stress causes mitochondrial fragmentation via differential modulation of mitochondrial fission-fusion proteins. Febs J. 2011; 278:941–954. [PubMed: 21232014]
20. Gan X, Huang S, Wu L, Wang Y, Hu G, Li G, Zhang H, Yu H, Swerdlow RH, Chen JX, Yan SS. Inhibition of ERK-DLP1 signaling and mitochondrial division alleviates mitochondrial dysfunction in Alzheimer's disease cybrid cell. Biochim Biophys Acta. 2014; 1842:220–231. [PubMed: 24252614]
21. Gan X, Wu L, Huang S, Zhong C, Shi H, Li G, Yu H, Howard Swerdlow R, Xi Chen J, Yan SS. Oxidative stress-mediated activation of extracellular signal-regulated kinase contributes to mild cognitive impairment-related mitochondrial dysfunction. Free Radic Biol Med. 2014; 75:230–240. [PubMed: 25064321]
22. Fan X, Hussien R, Brooks GA. H_2O_2-induced mitochondrial fragmentation in C2C12 myocytes. Free Radic Biol Med. 2010; 49:1646–1654. [PubMed: 20801212]
23. Yu TZ, Robotham JL, Yoon Y. Increased production of reactive oxygen species in hyperglycemic conditions requires dynamic change of mitochondrial morphology. Proc Natl Acad Sci U S A. 2006; 103:2653–2658. [PubMed: 16477035]
24. Yang YH, Li B, Zheng XF, Chen JW, Chen K, Jiang SD, Jiang LS. Oxidative damage to osteoblasts can be alleviated by early autophagy through the endoplasmic reticulum stress pathway-Implications for the treatment of osteoporosis. Free Radic Bio Med. 2014; 77:10–20. [PubMed: 25224042]
25. Westermann B. Mitochondrial fusion and fission in cell life and death. Nat Rev Mol Cell Biol. 2010; 11:872–884. [PubMed: 21102612]
26. Yoon Y, Galloway CA, Jhun BS, Yu TZ. Mitochondrial dynamics in diabetes. Antioxid Redox Signal. 2011; 14:439–457. [PubMed: 20518704]
27. Liesa M, Palacin M, Zorzano A. Mitochondrial dynamics in mammalian health and disease. Physiol Rev. 2009; 89:799–845. [PubMed: 19584314]
28. Manolagas SC. Birth and death of bone cells: basic regulatory mechanisms and implications for the pathogenesis and treatment of osteoporosis. Endocr Rev. 2000; 21:115–137. [PubMed: 10782361]

29. Gan XQ, Huang SB, Liu Y, Yan SS, Yu HY. The potential role of damage-associated molecular patterns derived from mitochondria in osteocyte apoptosis and bone remodeling. Bone. 2014; 62:67–68. [PubMed: 24503211]

30. Stambough JL, Brighton CT, Iannotti JP, Storey BT. Characterization of growth plate mitochondria. J Orthop Res Off Publ Orthop Res Soc. 1984; 2:235–246.

31. Wuthier RE, Chin JE, Hale JE, Register TC, Hale LV, Ishikawa Y. Isolation and characterization of calcium-accumulating matrix vesicles from chondrocytes of chicken epiphyseal growth plate cartilage in primary culture. J Biol Chem. 1985; 260:15972–15979. [PubMed: 3905800]

32. Zhang Z, Zheng L, Zhao Z, Shi J, Wang X, Huang J. Grape seed proanthocyanidins inhibit H_2O_2-induced osteoblastic MC3T3-E1 cell apoptosis via ameliorating H_2O_2-induced mitochondrial dysfunction. J Toxicol Sci. 2014; 39:803–813. [PubMed: 25242411]

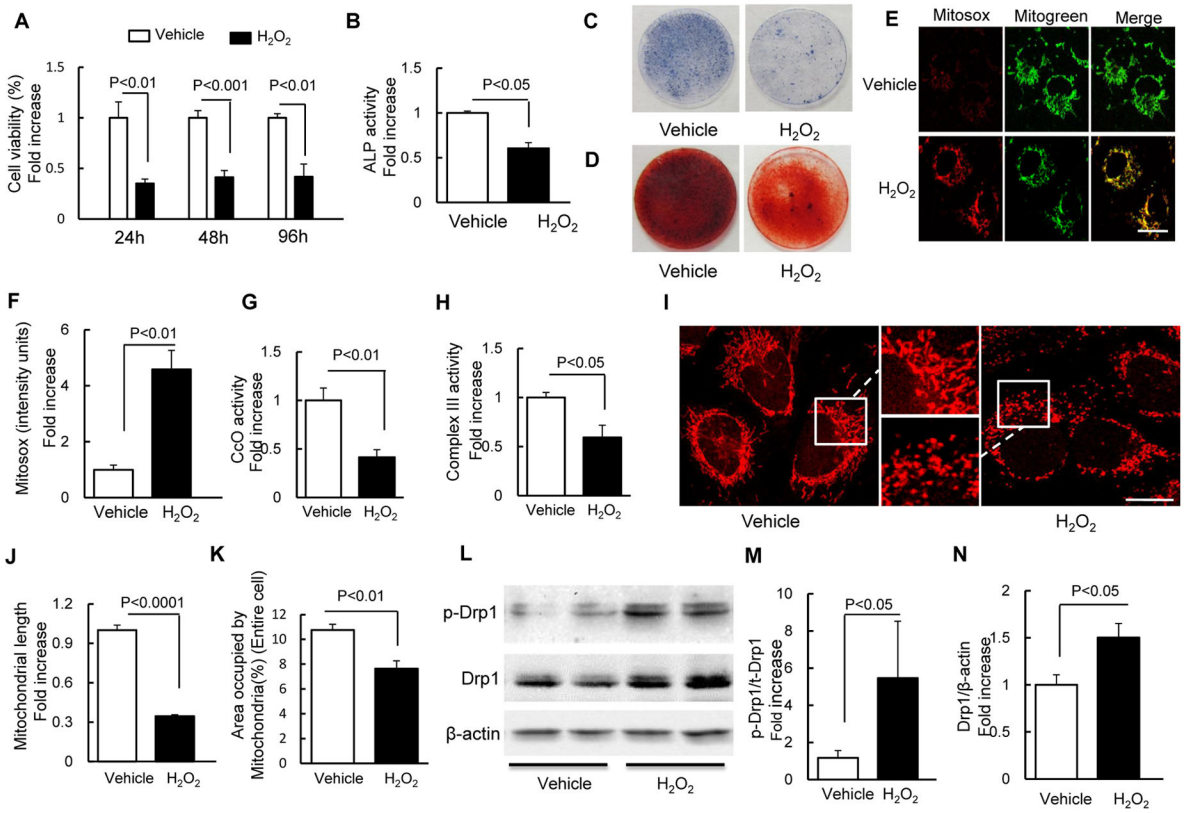

Fig. 1.

H_2O_2 induced osteoblast dysfunction. (A) Cell viability determined by MTT reduction in osteoblasts in the presence of H_2O_2. (B) ALP activity tested in osteoblasts as indicated groups. Data are expressed as fold increase relative to vehicle-treated cell. (C) ALP and (D) Alizarin red staining of osteoblasts in the indicated treatment groups. (E) Representative images with Mitosox staining. Mitogreen staining was used to show mitochondria (Scale bar = 10 μm). (F) Quantification of staining intensity for Mitosox staining. CcO activity (G) and Complex III activity (H) were measured in the indicated groups of cells. (I) Representative images for Mitotracker red staining to reveal mitochondrial morphology. The middle panel is a larger image corresponding to the indicated image on the left and right one (Scale bar = 5 μm). (J–K) Quantification of mitochondrial morphology in regard to mitochondrial length (J) and density of area occupied by mitochondria (K). (L) Representative immunoblots of phospho-Drp1 (p-Drp1) and total Drp1 (Drp1).(E–F) Quantification of immunoreactive bands for p-Drp1 relative to Drp1(M), Drp1 relative to β-actin(N) in osteoblast in the presence of H_2O_2 or vehicle treatment using NIH Image J software. Date are expressed as fold increase relative to vehicle treated cell.

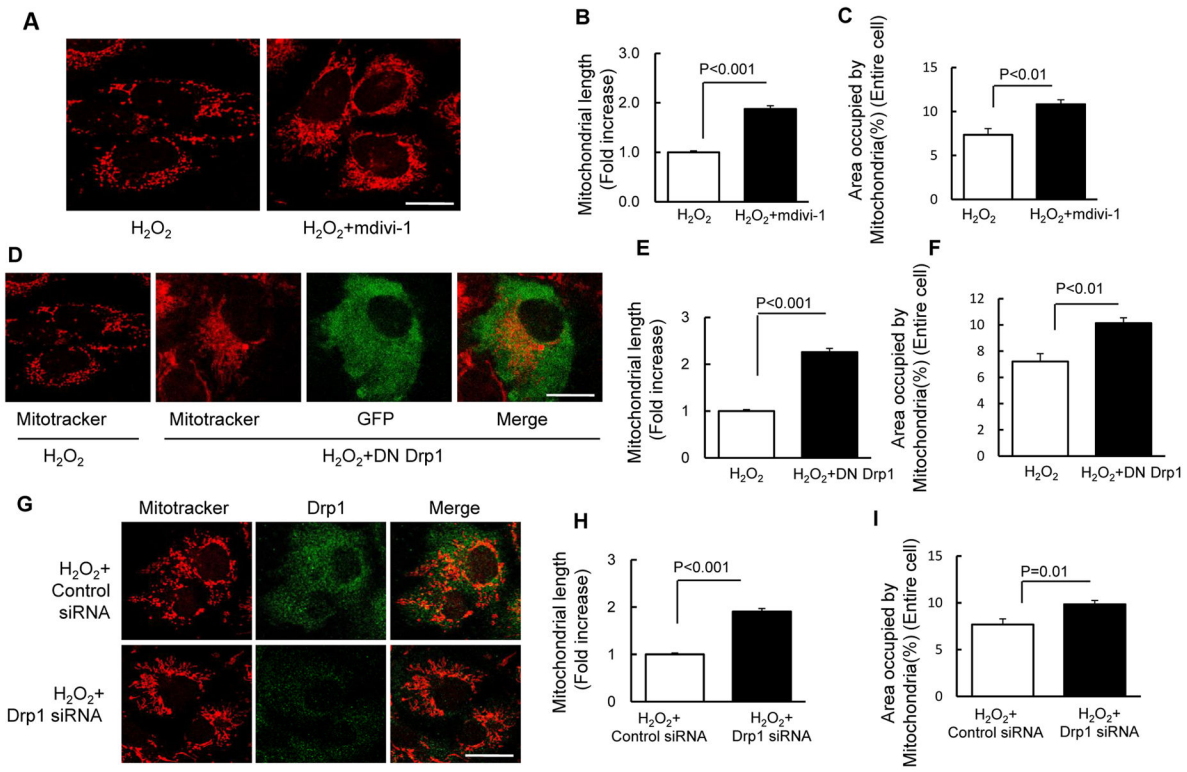

Fig. 2.

Drp1 inhibitor and Drp1 deficiency attenuated H_2O_2-induced osteoblast mitochondrial fragmentation. (A) Representative images with Mitotracker staining (Scale bar = 10 μm) of osteoblast treated with H_2O_2 with or without mdivi-1. (B–C) Quantification of mitochondrial morphology in regard to mitochondrial length (B) and density (C). (D) Representative images with Mitotracker staining (Scale bar = 10 μm) of osteoblast transfected with DN Drp1 and vector GFP. (E–F) Quantification of mitochondrial morphology including mitochondrial length (E) and density (F). (G) Representative images with Mitotracker staining (Scale bar = 10 μm) of osteoblast transfected with Drp1 siRNA and control siRNA. (H–I) Quantification of mitochondrial morphology including mitochondrial length (H) and density (I). Data are expressed as fold increase relative to vehicle treated cell.

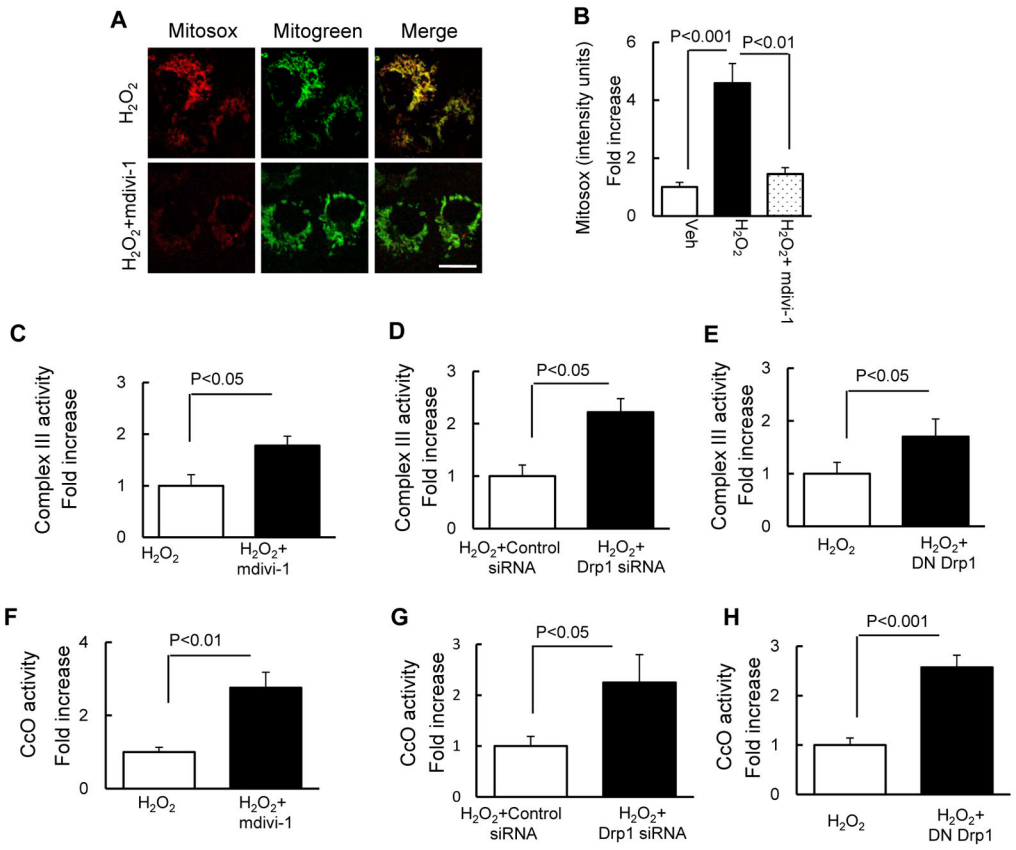

Fig. 3.

Drp1 inhibitor and Drp1deficiency attenuated H_2O_2-induced osteoblast mitochondrial dysfunction. (A) Representative images with Mitosox staining (Scale bar = 10 μm). Mitotracker staining was used to show mitochondria. Quantification of staining intensity for Mitosox (B) in the indicated groups of cells using NIH Image J software. Data are expressed as fold increase relative to vehicle treated cell. Complex III (C–E) and CcO (F–H) activity were measured in the indicated groups of cells. Data are expressed as fold increase relative to vehicle-treated cells.

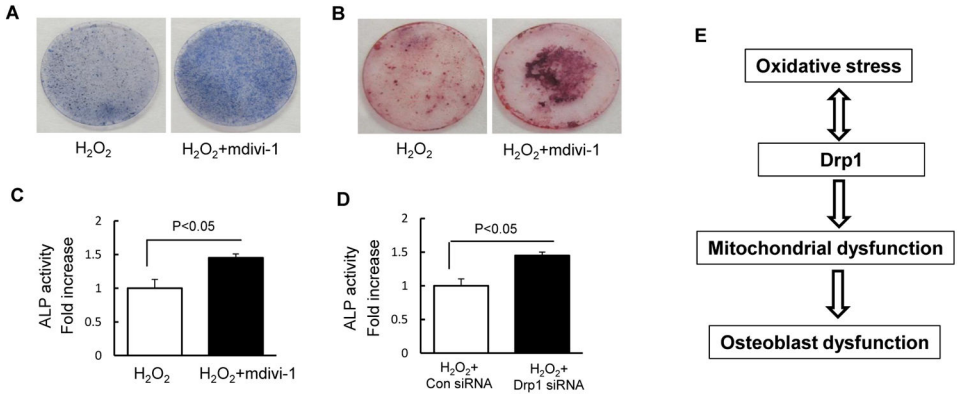

Fig. 4.

Drp1inhibitor and Drp1 deficiency attenuated H_2O_2-induced osteoblast dysfunction. (A) ALP and Alizarin red staining (B) of osteoblast in indicated treatment groups. (C–D) ALP activity was measured in osteoblast as the indicated groups. Data are expressed as fold increase relative to vehicle treated cell. (E) Working hypothesis: oxidative stress induces an increase in phosphorylation of Drp1 leading to mitochondrial dysfunction, which contributes to osteoblast dysfunction.